Discontinuities in Driven Spin-Boson Systems due to Coherent Destruction of Tunneling: Breakdown of the Floquet-Gibbs Distribution

Georg Engelhardt,[1] Gloria Platero,[2] and Jianshu Cao[1,3,*]
[1]Beijing Computational Science Research Center, Beijing 100193, People's Republic of China
[2]Instituto de Ciencia de Materiales de Madrid, CSIC, 28049 Madrid, Spain
[3]Department of Chemistry, Massachusetts Institute of Technology, 77 Massachusetts Avenue, Cambridge, Massachusetts 02139, USA

(Received 5 March 2019; published 20 September 2019)

If an open quantum system is periodically driven with high frequency and the driving commutes with the system-bath coupling operator, it is known that the system approaches a Floquet-Gibbs state, a generalization of Gibbs states to periodically driven systems. Here, we investigate the stationary state of an ac-driven system when the driving and dissipation are noncommutative. Then, the resulting stationary state does not obey the Floquet-Gibbs distribution, and the system dynamics is determined by inelastic scattering processes of the driving field. Based on the Floquet-Redfield formalism, we show that the probability distribution can exhibit population inversion and discontinuities, i.e., jumps, for parameters at which coherent destruction of tunneling takes place. These discontinuities can be observed as intensity jumps in the emission into the bath.

DOI: 10.1103/PhysRevLett.123.120602

Introduction.—Because of the precise experimental control, periodic driving has become a flexible tool for quantum state manipulation with extensive applications, e.g., quantum phase transitions, quantum transport, and even-harmonic generation [1–14]. The study of periodic driving becomes more interesting and challenging as the limit of light-matter coupling gets continuously pushed to the ultrastrong coupling regime [15].

As a quantum system is never completely decoupled from its environment, thermalization finally leads to relaxation towards a stationary state. Yet, relatively little is known about possible stationary states of periodically driven systems. In two recent articles, Shirai *et al.* have discussed conditions for effective Floquet-Gibbs states [16,17]. The probabilities of the Floquet states, characteristic states of periodically driven systems, are determined by their corresponding quasienergies ϵ_λ in a Gibbs-like fashion; thus, $p_\lambda \propto e^{-\beta\epsilon_\lambda}$. However, given the richness of quantum effects in periodically driven systems, the stationary states in these systems can deviate from Floquet-Gibbs states and can exhibit intriguing features [18–20].

Taking a driven two-level system coupled to the environment [Fig. 1(a)] as an example, there are additional processes which drive the system away from a Floquet-Gibbs state. Besides the usual transitions between the Floquet states $|\varphi_{n,\lambda}\rangle$ within a Brillouin zone n [marked in Fig. 1(a) with $A_{ij}^{(0)}$], there are additional transitions which are accompanied by emitting or absorbing a phonon (or photon) to the environment (marked with $A_{ij}^{(-1)}$). The phonon can have one of the following frequencies: $\Omega - \Delta$ ($|\varphi_{n,0}\rangle \to |\varphi_{n-1,1}\rangle$), Ω ($|\varphi_{n,0}\rangle \to |\varphi_{n-1,0}\rangle$ and $|\varphi_{n,1}\rangle \to |\varphi_{n-1,1}\rangle$), and $\Omega + \Delta$ ($|\varphi_{n,1}\rangle \to |\varphi_{n-1,0}\rangle$). Here, Ω denotes the driving frequency, and Δ denotes the difference between two quasienergies. Thus, the monochromatic driving field is scattered into three contributions. This emission is related to the Mollow triplet [21–24], appearing for scattering of a driving field closely in resonance with the level splitting. In contrast, here we focus on the fast driving regime. The emitted phonons can be blueshifted, unshifted, or redshifted, respectively. The unshifted transitions do not change the system state, but the shifted transitions can have a considerable influence on the dynamics.

In coherent destruction of tunneling (CDT) [25], the transition between two quantum states can be suppressed due to a destructive interplay of coherent wave dynamics and external periodic driving [26–28]. This genuine quantum localization appears at special ratios of the driving amplitude and frequency, which are associated with roots

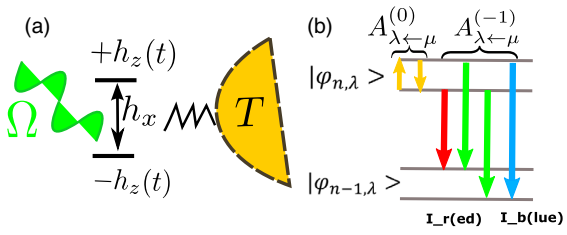

FIG. 1. (a) The ac-driven spin-boson model. Because of the coherent dynamics, it emits phonons with Ω, $\Omega \pm \Delta$ (unshifted, blueshifted, and redshifted), respectively. The corresponding transitions are depicted in (b).

of the Bessel function. CDT has been experimentally verified in Bose-Einstein condensates [29], optical waveguides [30], Fermi liquids [31], chaotic microcavities [32], and superconducting quantum circuits [33].

This Letter studies exotic stationary states appearing for weak system-bath coupling. The key difference from previous studies is the noncommutative coupling, which leads to exotic non-Gibbs distributions. In particular, we discover exotic discontinuities in the stationary state when smoothly increasing the driving amplitude. These jumps are a consequence of the CDT and can therefore appear in various systems. We explain how this counterintuitive feature is manifested in the emission of the driven system.

Model system.—We consider a spin-boson model consisting of a two-level system coupled to a thermal environment. In general, two-level systems are idealizations of more complicated level structures. The spin-boson model is a minimal model for quantum dissipation and exhibits quantum phenomena, including heat transfer, dissipative tunneling, and quantum phase transitions [34,35]. Adding an ac drive allows us to investigate spectroscopic properties. In a recent article, Maggazzù *et al.* have experimentally implemented an ac-driven spin-boson model in a superconducting quantum circuit [33]. Also, intriguing physical effects have been theoretically investigated in Refs. [36–42].

The Hamiltonian of the driven spin-boson model reads

$$H(t) = \frac{h_x}{2}\sigma_x + \frac{h_z(t)}{2}\sigma_z + \hat{\sigma}_\theta \sum_k V_k(b_k + b_k^\dagger) + H_B, \quad (1)$$

where σ_α with $\alpha = \{x, y, z\}$ denote the Pauli matrices, h_x denotes the tunneling amplitude, and $h_z(t) = h_{z,0} + h_{z,1}\cos(\Omega t)$ is the time-dependent on-site energy, where $h_{z,0}$ is the offset, $h_{z,1}$ is the driving amplitude, and Ω is the driving frequency. The bath $H_B = \sum_k \omega_k b_k^\dagger b_k$ with phonon frequencies ω_k is quadratic in bosonic operators b_k and is coupled via the system operator $\hat{\sigma}_\theta = \sin\theta\sigma_x + \cos\theta\sigma_z$ with strength V_k. Depending on the coupling angle θ, undriven and driven systems can give rise to diverse physical behavior [19,20,43–46].

Floquet theory describes the dynamics of periodically driven systems [47,48]. Because of the driving with a period of $\tau = 2\pi/\Omega$, the characteristic states of the system fulfill $|\Phi_{n,\lambda}(t)\rangle = e^{-i\epsilon_{n,\lambda}t}|\varphi_{n,\lambda}(t)\rangle$, with quasienergy $\epsilon_{n,\lambda}$ and periodic Floquet state $|\varphi_{n,\lambda}(t)\rangle = |\varphi_{n,\lambda}(t+\tau)\rangle$. These states are the analog to the eigenstates in time-independent systems. The Floquet states λ are not uniquely defined due to the Brillouin zone index n: A state with index n can be related to the $n = 0$ state by $\epsilon_{n,\lambda} = \epsilon_{0,\lambda} + n\Omega$ and $|\varphi_{n,\lambda}(t)\rangle = e^{-in\Omega t}|\varphi_{0,\lambda}(t)\rangle$. The stroboscopic Floquet states are the eigenstates of the time-evolution operator after one period $\hat{U}_s(\tau)|\varphi_{n,\lambda}(0)\rangle = e^{-i\epsilon_{n,\lambda}\tau}|\varphi_{n,\lambda}(0)\rangle$.

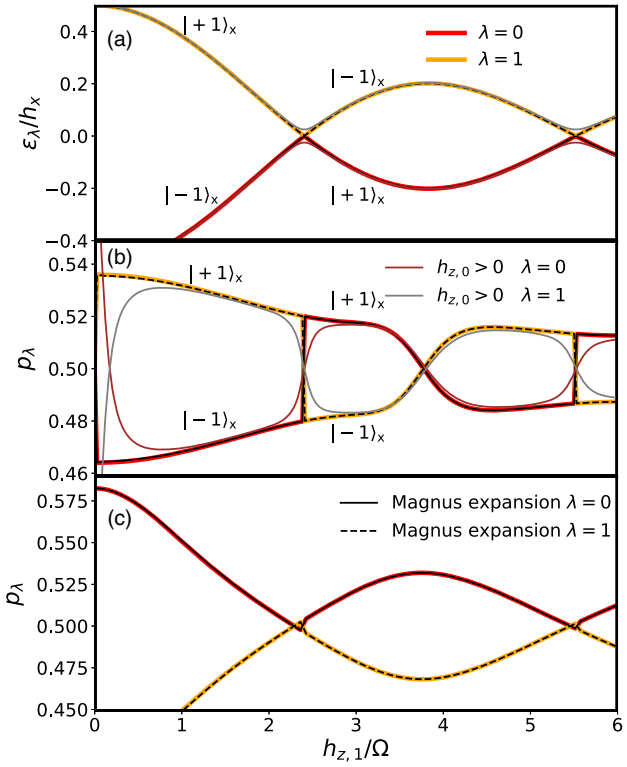

FIG. 2. (a) Quasienergy spectrum as a function of the driving amplitude $h_{z,1}$. (b) and (c) depict the probabilities p_λ for $\theta = \pi/2$ ($\hat{\sigma}_{\pi/2} = \sigma_x$) and $\theta = \pi/4$ ($\hat{\sigma}_{\pi/4} = (1/\sqrt{2})\sigma_x + (1/\sqrt{2})\sigma_z$), respectively. The Floquet states are approximately given by the eigenstates of σ_x, which we denote by $|-1\rangle_x$ and $|+1\rangle_x$ corresponding to eigenvalues -1 and 1, respectively. We choose $h_{z,0} = 0$ [except for the thin lines in (b), where $h_{z,0} = 0.05h_x$], $\omega_c = 10h_x$, $\Omega = 40h_x$, and $k_BT = 3h_x$. All results are presented in a γ-independent way.

In Fig. 2(a), we depict the quasienergies $\epsilon_\lambda = \epsilon_{0,\lambda}$ of the isolated two-level system as a function of $h_{z,1}/\Omega$, where $\lambda = 0$, 1 and $n = 0$. The stroboscopic dynamics follows the effective Hamiltonian $H_{\text{eff}} = (h_{z,0}/2)\sigma_z + (h_x/2)\mathcal{J}_0(h_{z,1}/\Omega)\sigma_x + \mathcal{O}(1/\Omega)$ [49]. For $h_{z,0} = 0$, we find $\epsilon_\lambda = \pm h_x\mathcal{J}_0(h_{z,1}/\Omega)/2$, so that there are degeneracies at the roots of the Bessel function $\mathcal{J}_0(h_{z,1}/\Omega) = 0$. This is the CDT effect, as the dynamics is frozen. The stroboscopic Floquet states read $|\varphi_\lambda(0)\rangle \approx |\text{sgn}[\mathcal{J}_0(h_{z,1}/\Omega)](-1)^\lambda\rangle_x$. Accordingly, there is a nonanalytic switch of the Floquet state, e.g., $|\varphi_0(0)\rangle = |-1\rangle_x$ to $|\varphi_0(0)\rangle = |+1\rangle_x$, at the roots of the Bessel function.

Rate equations.—An important point to realize is that, though the states $|\varphi_{n,\lambda}(t)\rangle$ of the two-level system are equivalent for different n in a closed system, n becomes physically relevant when the system is coupled to a bath H_B. The bath can trigger transitions between different Brillouin zones n, n'. In Fig. 1(b), we illustrate transitions associated with $\Delta n = n - n' \in \{0, -1\}$. Using the secular Floquet-Redfield formalism [18,48,50], one can derive the rate equations

$$\frac{d}{dt}p_0 = -\sum_{\Delta n} A^{(\Delta n)}_{1\leftarrow 0} p_0 + \sum_{\Delta n} A^{(\Delta n)}_{0\leftarrow 1} p_1,$$
$$\frac{d}{dt}p_1 = +\sum_{\Delta n} A^{(\Delta n)}_{1\leftarrow 0} p_0 - \sum_{\Delta n} A^{(\Delta n)}_{0\leftarrow 1} p_1, \tag{2}$$

where p_λ denotes the probability to be in Floquet state λ and $A^{(n)}_{\lambda\leftarrow\mu}$ is the transition probability between two Floquet states:

$$A^{(n)}_{\lambda\leftarrow\mu} = \Gamma(\Delta^n_{\lambda\mu})[n_B(\Delta^n_{\lambda\mu})+1]|a^n_{\lambda\leftarrow\mu}|^2,$$
$$a^{(n)}_{\lambda\leftarrow\mu} = \frac{1}{\tau}\int_0^\tau \langle\varphi_\lambda(0)|\hat{\sigma}_\theta(t)|\varphi_\mu(0)\rangle e^{-in\Omega t}dt. \tag{3}$$

Here, $n_B(\omega)$ denotes the Bose distribution, $\Gamma(\omega) = \sum_k V_k^2\delta(\omega-\omega_k) = \gamma\omega/(\omega^2+\omega_c^2)$ (coupling strength γ and cutoff frequency ω_c) denotes the coupling density, defined for negative frequencies by $\Gamma(\omega) = -\Gamma(-\omega)$, and $\Delta^n_{\lambda\mu} = \epsilon_\mu - \epsilon_\lambda - n\Omega$. The time-dependent operator reads $\hat{\sigma}_\theta(t) = e^{i\hat{\Lambda}(t)}\hat{\sigma}_\theta e^{-i\hat{\Lambda}(t)}$, where $\hat{\Lambda}(t)$ is defined by the Floquet states $|\varphi_\lambda(t)\rangle = e^{-i\hat{\Lambda}(t)}|\varphi_\lambda(0)\rangle$.

It is easy to show that the rates obey the detailed balance condition $A^{(n)}_{\lambda\leftarrow\mu} = A^{(-n)}_{\mu\leftarrow\lambda}e^{\Delta^{(n)}_\mu/T}$, where T is the temperature of the environment. In general, the $A^{(n)}_{\lambda\leftarrow\mu}$ do not fulfill the detailed balance condition, which gives rise to a breakdown of a Gibbs-like state; thus, $p_0/p_1 \neq e^{-(\epsilon_1-\epsilon_0)/T}$.

Stationary state.—In the Floquet-Redfield formalism, the stationary density matrix reads $\rho_s(t) = \sum_\lambda p_\lambda|\varphi_\lambda(t)\rangle\langle\varphi_\lambda(t)|$, which is time periodic. For $\theta = 0$, the system approaches a Floquet-Gibbs state according to Ref. [17], as the rates $A^{(n\neq 0)}_{\lambda\leftarrow\mu} \approx 0$ and the rates $A^{(0)}_{\lambda\leftarrow\mu}$ keep the detailed balance condition. This happens as, for $\theta = 0$, the driving operator and system-bath coupling commute [17].

Figures 2(b) and 2(c) depict the stationary state for $\theta = \pi/2$ and $\pi/4$, respectively. In Fig. 2(b), we find a probability inversion for small $h_{z,1}/\Omega$ and probability jumps at the roots of the Bessel function $\mathcal{J}_0(h_{z,1}/\Omega) = 0$. Because of a generalized parity symmetry, $A^{(0)}_{\lambda\leftarrow\mu}$ vanishes exactly [51]. Consequently, the rate equations are dominated by the transitions $\Delta n = -1$, as $n_B(|\Delta^{n>0}_{\lambda\mu}|) \ll 1$ due to large $\Delta^n_{\lambda,\mu} \approx -n\Omega$. These transitions are marked by the red and blue arrows in Fig. 1(b) (green transitions do not change the state). The corresponding coefficients $|a^{(-1)}_{\mu\leftarrow\lambda}|$ are depicted in Fig. 3(a), where we observe that $|a^{(-1)}_{1\leftarrow 0}| > |a^{(-1)}_{0\leftarrow 1}|$ for, e.g., $h_{z,1}/\Omega < z_0$, with z_0 denoting the first root of the zeroth-order Bessel function. As $n_B(\Delta^{n\neq 0}_{\lambda\mu}) \ll 1$ and $\Gamma(\Delta^{(-1)}_{10}) \approx \Gamma(\Delta^{(-1)}_{01})$, we find from Eq. (2) that $p_1/p_0 \approx |a^{(-1)}_{1\leftarrow 0}|^2/|a^{(-1)}_{0\leftarrow 1}|^2$, which explains the probability inversion. The rates explain the jump in the probability distribution. In Fig. 3(a), we observe jumps at the CDT positions, which are magnified in Fig. 3(b). The noncontinuous behavior becomes more clear when considering Eq. (3). At the CDT, the Floquet states switch, thus, $|\varphi_\lambda(0)\rangle \leftrightarrow |\varphi_\mu(0)\rangle$, which gives rise to the nonanalytic behavior.

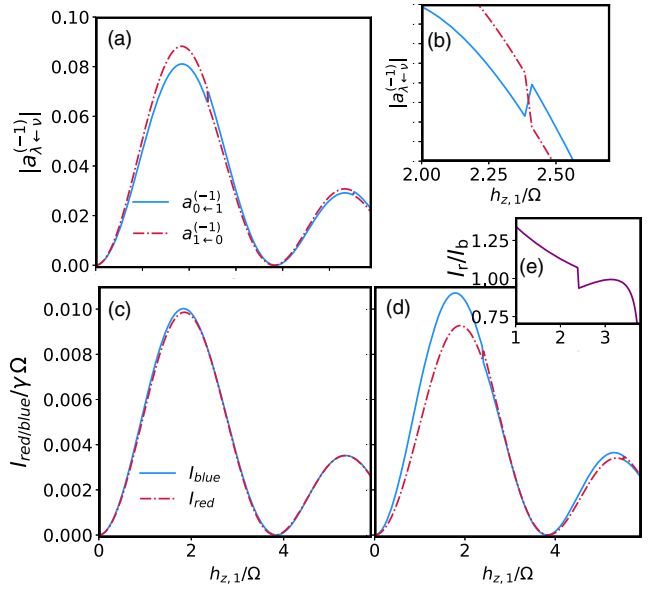

FIG. 3. (a) The transition coefficients for $\hat{\sigma}_{\pi/2}$. The coefficients for $\hat{\sigma}_{\pi/4}$ are almost equal. (b) Magnification of the jump discontinuity in (a). (c) and (d) depict corresponding intensities of blue- and redshifted emitted phonons for $\theta = \pi/2$ and $\theta = \pi/4$ coupling, respectively. The ratio of the red- and blueshifted emission intensities for $\theta = \pi/4$ is depicted in (e). Parameters are the same as in Fig. 2.

A similar reasoning can be applied to the $\hat{\sigma}_{\pi/4}$ coupling depicted in Fig. 2(c). Away from the CDT, the probability distribution mainly corresponds to the Floquet-Gibbs state: The coupling $\hat{\sigma}_{\pi/4}$ has a σ_z contribution so that the rates $A^{(0)}_{\lambda\leftarrow\mu} \gg A^{(-1)}_{\lambda\leftarrow\mu}$ are close to a Gibbs state. However, the coefficients $a^{(-1)}_{\lambda\leftarrow\mu}$ are almost equal to those of the $\hat{\sigma}_{\pi/2}$ case giving rise to a probability jump, yet to a very small extent.

Importantly, although there is a jump discontinuity, the density matrix remains continuous as a function of $h_{z,1}$, as the stationary density matrix $\rho_s(t) = \sum_\lambda p_\lambda|\varphi_\lambda(t)\rangle\langle\varphi_\lambda(t)|$ exhibits a simultaneous switch of p_λ and $|\varphi_\lambda(t)\rangle$. Yet, the probability jump does not depend on how the states $\lambda = 0$, 1 are labeled, as the labeling can be uniquely defined for finite $h_{z,0} \to 0$. A corresponding quasienergy spectrum is depicted in Fig. 2(a) with thin lines. For finite but small $h_{z,0}$, the gap closing is released as depicted in Fig. 2(a). Accordingly, the states depend smoothly on $h_{z,1}$, so that the p_λ are also uniquely defined as can be observed in Fig. 2(b). The ordering of the states $\lambda = 0$, 1 can be thus uniquely defined in terms of the limit $h_{z,0} \to 0$. Moreover, quantum state tomography of the stationary state for small $h_{z,0} \to 0$ can experimentally reveal the jump.

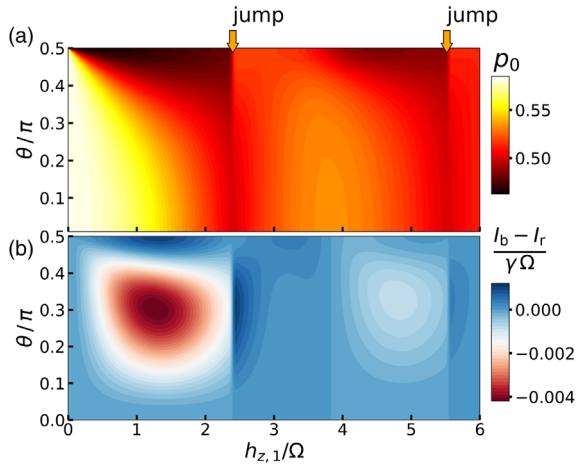

FIG. 4. (a) shows the probability of the Floquet state $|\varphi_0\rangle$ in a stationary state of the Hamiltonian Eq. (1). (b) depicts the difference of the blue- and redshifted emission intensities into the bath. Parameters are the same as in Fig. 2.

The interplay of θ and $h_{z,1}$ can be fully analyzed in Fig. 4(a), where the stationary state strongly depends on θ, though the system is only weakly coupled to the environment. In particular, for $\theta \approx 0.5\pi$ and small $h_{z,1}$, we find inversion: $p_0 < 0.5$; thus, there is a strong deviation from the Floquet-Gibbs state, appearing for $\theta = 0$.

Phonon emission.—The nonanalytic behavior of the probabilities can be observed in the emission. Every transition $A^{(-1)}_{\lambda\leftarrow\mu}$ is related to the emission of phonons with an energy of either Ω or $\Omega \pm \Delta$. The corresponding intensities $I_{b,r} = I(\Omega \pm \Delta)$ are given by $I_b = (\Omega + \epsilon_1 - \epsilon_0)A^{(-1)}_{0\leftarrow 1}p_1$ and $I_r = (\Omega - \epsilon_1 + \epsilon_0)A^{(-1)}_{1\leftarrow 0}p_0$. We depict the blue- and redshifted intensities in Figs. 3(c) and 3(d). For $\hat{\sigma}_{\pi/2}$, we observe that the two intensities are almost equal. As the stationary state is governed by the rates $A^{(-1)}_{\lambda\leftarrow\nu}$, we find $p_0 \propto A^{(-1)}_{0\leftarrow 1}$ and $p_1 \propto A^{(-1)}_{1\leftarrow 0}$, so that $I_r \approx I_b$ for high-frequency $\Omega \gg \epsilon_1 - \epsilon_0$.

For $\hat{\sigma}_0 = \sigma_z$, at which the system approaches a Floquet-Gibbs state, it is known that the rates $A^{(n\neq 0)}_{\mu\leftarrow\nu} \approx 0$ [16]. Consequently, here both $I_{r/b}$ vanish. Considering the difference $I_b - I_r$ in Fig. 4(b), we consequently find that the difference is smooth in $h_{z,1}$ for both limiting cases $\theta = 0,\ \pi/2$. However, in between there is a significant jump, which is the strongest for about $\theta \approx 0.3\pi$.

Let us consider the $\hat{\sigma}_{\pi/4}$ coupling. Because of the σ_z coupling component, the $A^{(0)}_{\lambda\leftarrow\nu}$ rates are dominant, which leads to an (almost) thermalization of the system with its environment. However, the rates $A^{(-1)}_{\lambda\leftarrow\nu}$ still exhibit a jump at the CDT, so that we find jumps in I_r and I_b, as can be observed in Fig. 3(d).

Magnus expansion.—To develop further insight, we evaluate the rates Eq. (3) using the Magnus expansion in a rotating frame for a high driving frequency [52,53]. Details can be found in the Supplemental Material [49]. We obtain

$$a^{(n)}_{\mu,\lambda} = \mathcal{S}^{(n)}_x\langle\sigma_x\rangle_{\mu\lambda} + i\cdot\mathcal{S}^{(n)}_y\langle\sigma_y\rangle_{\mu\lambda} + \mathcal{S}^{(n)}_z\langle\sigma_z\rangle_{\mu\lambda}, \quad (4)$$

where we have defined $\langle\sigma_\alpha\rangle_{\mu\lambda} = \langle\varphi_\mu(0)|\sigma_\alpha|\varphi_\lambda(0)\rangle$. The coefficients $\mathcal{S}^{(n)}_\alpha$ depend on the system parameters and, importantly, are real valued.

TABLE I. Transition coefficients $a^{(n)}_{\mu,\lambda}$ of all possible transitions between different Floquet states $|\varphi_\lambda(0)\rangle$.

$n = 0$	$\|-1\rangle_x$	$\|+1\rangle_x$
$\|-1\rangle_x$	$\mathcal{S}^{(0)}_x$	$\mathcal{S}^{(0)}_z$
$\|+1\rangle_x$	$\mathcal{S}^{(0)}_z$	$-\mathcal{S}^{(0)}_x$
$n = -1$	$\|-1\rangle_x$	$\|+1\rangle_x$
$\|-1\rangle_x$	$\mathcal{S}^{(-1)}_x$	$\mathcal{S}^{(-1)}_y + \mathcal{S}^{(-1)}_z$
$\|+1\rangle_x$	$\mathcal{S}^{(-1)}_y - \mathcal{S}^{(-1)}_z$	$-\mathcal{S}^{(-1)}_x$

The $a^{(n)}_{\mu,\lambda}$ are evaluated in Table I. Because of a symmetry condition, some of the $\mathcal{S}^{(n)}_\alpha$ vanish exactly. For $n = 0$, we find a Hermitian structure for the eigenstates $|\varphi_\lambda(0)\rangle \approx |-1\rangle_x, |+1\rangle_x$, which are mainly determined by $H^{(0)}_{\text{eff}} \propto \sigma_x$. For $n = -1$, the transition coefficients are dominated by $\mathcal{S}^{(-1)}_y \propto \mathcal{J}_{-1}(h_{z,1}/\Omega)$, which explains the oscillations in Fig. 3(a). Importantly, they do not exhibit a Hermitian structure. This leads to a breakdown of the detailed balance relation and gives rise to the jumps in Figs. 2(b) and 2(c). This appears as $|\varphi_0(0)\rangle$ switches from $|-1\rangle_x$ to $|+1\rangle_x$ and, simultaneously, $|\varphi_1(0)\rangle$ switches from $|+1\rangle_x$ to $|-1\rangle_x$, causing a jump of $a^{(-1)}_{\mu,\lambda}$.

We can use Eq. (4) to understand the intensity jump. Expanding around a root z_0 of the Bessel function $\mathcal{J}_0(z_0) \approx 0$, we find $I_{\text{red}}/I_{\text{blue}} \approx 1 \pm 2(h_x/\Omega)\alpha$ with a constant α and $\pm$ for $h_{z,1}/\Omega \lessgtr z_0$. Interestingly, the effect scales as $1/\Omega$ near the CDT [Fig. 3(e)].

Discussion.—The CDT in a driven dissipative system gives rise to surprising effects. The presence of a bath can give rise to inversion and jumps due to CDT in the probability distribution of the Floquet state. As there is a simultaneous discontinuity of Floquet states, the reduced density matrix remains continuous. Consequently, the probability jumps cannot be detected in system observables. Yet, precursors of the jump can be observed when the driving has a constant offset (thin lines in Fig. 2). Moreover, the jump behavior has a consequence on the emission, such that the blue- and redshifted intensities can exhibit a discontinuity at the CDT. This can be measured by phonon spectroscopy. For our parameters, the ratio of the shifted intensities exhibits a jump of about 10%.

The underlying reason for these discontinuities is a crossing of the Floquet states at the CDT. This causes a jump in the transition coefficients of the rates in Eq. (3). Consequently, the effect does not depend on the details of the bath. Yet, the system-bath coupling operator is important. For a $\hat{\sigma}_0 = \sigma_z$ coupling as investigated in Ref. [16], the stationary density matrix of the system recovers the Floquet-Gibbs states. For $\hat{\sigma}_{\pi/2} = \sigma_x$, we find extreme deviations from the Floquet-Gibbs state with probability inversion as observed in Fig. 2(b). With this noncommutative coupling, the probability jump at the CDT turns out to be most significant. However, there is no signature in the frequency-shifted intensities. For $\hat{\sigma}_{\pi/4}$ coupling, though the probability jumps are very small, there is a clear jump discontinuity in the blue- and redshifted intensity.

The noncontinuous behavior is general. First, it is not a consequence of the high-frequency regime, which we considered here to obtain analytical calculations. The CDT appears due to an exact degeneracy of the quasienergies which is persistent even for very low driving frequencies [48]. Consequently, the jump behavior could remain when lowering the driving frequency. Second, our findings are not restricted to the dissipative two-level system. Similar probability jumps could also be observed in a dissipative driven Lipikin-Meshkov-Glick model, which gives rise to many-body CDT [52]. Furthermore, these findings will be important for electronic transport [54–56]. It will be interesting to explore the fate of the jumps for stronger environmental coupling using methods such as in Refs. [57–62].

Periodic driving provides a flexible but highly controllable tool to manipulate quantum systems. Given the findings in this Letter, one could employ the jump effect to create transistorlike switches, as the frequency-shifted intensities sensitively depend on the driving amplitude. Because of the various driving modes and the extensive parameter space, it is not surprising that the probability jumps remained undiscovered. For instance, when the driving force is a rotating field and, thus, $\cos(\Omega t)\sigma_x + \sin(\Omega t)\sigma_y$ as in Refs. [39–41], the probabilities jumps do not appear, as the system does not exhibit CDT.

G. E. gratefully acknowledges financial support from the China Postdoc Science Foundation (Grant No. 2018M640054), J. C. acknowledges support from the NSF (Grants No. CHE 1800301 and No. CHE 1836913). Both acknowledge the Natural Science Foundation of China (under Grant No. U1930402). G. P. acknowledges MINECO (Grant No. MAT2017-86717-P) and support from CSIC Research Platform PTI-001. G. P. also acknowledges support from the DFG within SBF 1277 and the "Unidad Asociada: Matemática Aplicadaa la teoría de la Materia Condensada" with the Carlos III University of Madrid. The authors thank Abraham Nitzan, Michael Thorwart, Sigmund Kohler, Hui Dong, and Tilen Čadež for inspiring discussions.

*jianshu@mit.edu

[1] M. Aidelsburger, M. Atala, M. Lohse, J. T. Barreiro, B. Paredes, and I. Bloch, Realization of the Hofstadter Hamiltonian with Ultracold Atoms in Optical Lattices, Phys. Rev. Lett. **111**, 185301 (2013).
[2] G. Jotzu, M. Messer, R. Desbuquois, M. Lebrat, T. Uehlinger, D. Greif, and T. Esslinger, Experimental realization of the topological Haldane model with ultracold fermions, Nature (London) **515**, 237 (2014).
[3] M. Benito, A. Gómez-León, V. M. Bastidas, T. Brandes, and G. Platero, Floquet engineering of long-range p-wave superconductivity, Phys. Rev. B **90**, 205127 (2014).
[4] G. Engelhardt, M. Benito, G. Platero, and T. Brandes, Topologically Enforced Bifurcations in Superconducting Circuits, Phys. Rev. Lett. **118**, 197702 (2017).
[5] V. M. Bastidas, C. Emary, B. Regler, and T. Brandes, Nonequilibrium Quantum Phase Transitions in the Dicke Model, Phys. Rev. Lett. **108**, 043003 (2012).
[6] G. Engelhardt, M. Benito, G. Platero, and T. Brandes, Topological Instabilities in Ac-Driven Bosonic Systems, Phys. Rev. Lett. **117**, 045302 (2016).
[7] G. Engelhardt, V. M. Bastidas, C. Emary, and T. Brandes, AC-driven quantum phase transition in the Lipkin-Meshkov-Glick model, Phys. Rev. E **87**, 052110 (2013).
[8] J. Liu, C.-Y. Hsieh, and J. Cao, Efficiency at maximum power of a quantum Carnot engine with temperature tunable baths, arXiv:1710.06565.
[9] G. Platero and R. Aguado, Photon-assisted transport in semiconductor nanostructures, Phys. Rep. **395**, 1 (2004).
[10] R. Bavli and H. Metiu, Properties of an electron in a quantum double well driven by a strong laser: Localization, low-frequency, and even-harmonic generation, Phys. Rev. A **47**, 3299 (1993).
[11] Y. Dakhnovskii and R. Bavli, Emission spectrum and localization of electrons in quantum-well systems induced by a strong laser field, Phys. Rev. B **48**, 11020 (1993).
[12] P. R. Graves and D. Gardiner, *Practical Raman Spectroscopy* (Springer, New York, 1989).
[13] N. Mann, M. R. Bakhtiari, F. Massel, A. Pelster, and M. Thorwart, Driven bose-hubbard model with a parametrically modulated harmonic trap, Phys. Rev. A **95**, 043604 (2017).
[14] A. Komnik and M. Thorwart, BCS theory of driven superconductivity, Eur. Phys. J. B **89**, 244 (2016).
[15] P. Forn-Díaz, L. Lamata, E. Rico, J. Kono, and E. Solano, Ultrastrong coupling regimes of light-matter interaction, Rev. Mod. Phys. **91**, 025005 (2019).
[16] T. Shirai, T. Mori, and S. Miyashita, Condition for emergence of the Floquet-Gibbs state in periodically driven open systems, Phys. Rev. E **91**, 030101(R) (2015).
[17] T. Shirai, J. Thingna, T. Mori, S. Denisov, P. Hänggi, and S. Miyashita, Effective FloquetGibbs states for dissipative quantum systems, New J. Phys. **18**, 053008 (2016).
[18] S. Kohler, R. Utermann, P. Hänggi, and T. Dittrich, Coherent and incoherent chaotic tunneling near singlet-doublet crossings, Phys. Rev. E **58**, 7219 (1998).
[19] R. Blattmann, P. Hänggi, and S. Kohler, Qubit interference at avoided crossings: The role of driving shape and bath coupling, Phys. Rev. A **91**, 042109 (2015).

[20] H. Kohler, A. Hackl, and S. Kehrein, Nonequilibrium dynamics of a system with quantum frustration, Phys. Rev. B **88**, 205122 (2013).

[21] B. R. Mollow, Power spectrum of light scattered by two-level systems, Phys. Rev. **188**, 1969 (1969).

[22] B. Pigeau, S. Rohr, L. M. De Lepinay, A. Gloppe, V. Jacques, and O. Arcizet, Observation of a phononic Mollow triplet in a multimode hybrid spin-nanomechanical system, Nat. Commun. **6**, 8603 (2015).

[23] Y. Yan, Z. Lu, and H. Zheng, Resonance fluorescence of strongly driven two-level system coupled to multiple dissipative reservoirs, Ann. Phys. (Amsterdam) **371**, 159 (2016).

[24] H. Chen, T. E. Li, A. Nitzan, and J. E. Subotnik, Predictive semiclassical model for coherent and incoherent emission in the strong field regime: The mollow triplet revisited, J. Phys. Chem. Lett. **10**, 1331 (2019).

[25] F. Grossmann, T. Dittrich, P. Jung, and P. Hänggi, Coherent Destruction of Tunneling, Phys. Rev. Lett. **67**, 516 (1991).

[26] M. Frasca, Perturbative results on localization for a driven two-level system, Phys. Rev. B **68**, 165315 (2003).

[27] J. T. Stockburger, Stabilizing coherent destruction of tunneling, Phys. Rev. E **59**, R4709 (1999).

[28] J. C. A. Barata and W. F. Wreszinski, Strong-Coupling Theory of Two-Level Atoms in Periodic Fields, Phys. Rev. Lett. **84**, 2112 (2000).

[29] E. Kierig, U. Schnorrberger, A. Schietinger, J. Tomkovic, and M. K. Oberthaler, Single-Particle Tunneling in Strongly Driven Double-Well Potentials, Phys. Rev. Lett. **100**, 190405 (2008).

[30] S. Mukherjee, M. Valiente, N. Goldman, A. Spracklen, E. Andersson, P. Öhberg, and R. R. Thomson, Observation of pair tunneling and coherent destruction of tunneling in arrays of optical waveguides, Phys. Rev. A **94**, 053853 (2016).

[31] A. Zenesini, H. Lignier, D. Ciampini, O. Morsch, and E. Arimondo, Coherent Control of Dressed Matter Waves, Phys. Rev. Lett. **102**, 100403 (2009).

[32] Q. Song, Z. Gu, S. Liu, and S. Xiao, Coherent destruction of tunneling in chaotic microcavities via three-state anticrossings, Sci. Rep. **4**, 4858 (2015).

[33] L. Magazzù, P. Forndiaz, R. Belyansky, J. L. Orgiazzi, M. A. Yurtalan, M. Otto, A. Lupascu, C. Wilson, and M. Grifoni, Probing the strongly driven spin-boson model in a superconducting quantum circuit, Nat. Commun. **9**, 1403 (2018).

[34] U. Weiss, *Quantum Dissipative Systems* (World Scientific, Singapore, 2012), Vol. 13.

[35] A. J. Leggett, S. Chakravarty, A. T. Dorsey, M. P. A. Fisher, A. Garg, and W. Zwerger, Dynamics of the dissipative two-state system, Rev. Mod. Phys. **59**, 1 (1987).

[36] V. Peano and M. Thorwart, Dynamics of the quantum Duffing oscillator in the driving induced bistable regime, Chem. Phys. **322**, 135 (2006), real-time dynamics in complex quantum systems.

[37] K. M. Fonseca-Romero, S. Kohler, and P. Hänggi, Coherence control for qubits, Chem. Phys. **296**, 307 (2004), the Spin-Boson Problem: From Electron Transfer to Quantum Computing … to the 60th Birthday of Professor Ulrich Weiss.

[38] J. Shao and P. Hänggi, Controlling quantum coherence by circularly polarized fields, Phys. Rev. A **56**, R4397 (1997).

[39] K. Szczygielski, D. Gelbwaser-Klimovsky, and R. Alicki, Markovian master equation and thermodynamics of a two-level system in a strong laser field, Phys. Rev. E **87**, 012120 (2013).

[40] R. Alicki, D. A. Lidar, and P. Zanardi, Internal consistency of fault-tolerant quantum error correction in light of rigorous derivations of the quantum markovian limit, Phys. Rev. A **73**, 052311 (2006).

[41] E. Geva, R. Kosloff, and J. L. Skinner, On the relaxation of a two-level system driven by a strong electromagnetic field, J. Chem. Phys. **102**, 8541 (1995).

[42] M. Grifoni, M. Sassetti, P. Hänggi, and U. Weiss, Cooperative effects in the nonlinearly driven spin-boson system, Phys. Rev. E **52**, 3596 (1995).

[43] C. Duan, C.-Y. Hsieh, J. Liu, and J. Cao, Unusual transport properties with non-commutative system-bath coupling operators, arXiv:1907.11262.

[44] A. H. Castro Neto, E. Novais, L. Borda, G. Zaránd, and I. Affleck, Quantum Magnetic Impurities in Magnetically Ordered Systems, Phys. Rev. Lett. **91**, 096401 (2003).

[45] C. Guo, A. Weichselbaum, J. von Delft, and M. Vojta, Critical and Strong-Coupling Phases in One- and Two-Bath Spin-Boson Models, Phys. Rev. Lett. **108**, 160401 (2012).

[46] B. Bruognolo, A. Weichselbaum, C. Guo, J. von Delft, I. Schneider, and M. Vojta, Two-bath spin-boson model: Phase diagram and critical properties, Phys. Rev. B **90**, 245130 (2014).

[47] J. H. Shirley, Solution of the Schrödinger equation with a Hamiltonian periodic in time, Phys. Rev. **138**, B979 (1965).

[48] M. Grifoni and P. Hänggi, Driven quantum tunneling, Phys. Rep. **304**, 229 (1998).

[49] See Supplemental Material at http://link.aps.org/supplemental/10.1103/PhysRevLett.123.120602 for a detailed derivation of the effective Hamiltonian and the transition coefficients in the Floquet-Redeld equation based on the Magnus expansion in the high frequency regime.

[50] J. C. L. Carreno, E. D. Valle, and F. P. Laussy, Photon correlations from the Mollow triplet, Laser Photonics Rev. **11**, 1700090 (2017).

[51] Because of $\sigma_z H_s(t)\sigma_z = H_s(t+\tau/2)$, the Floquet states fulfill $\sigma_z|\phi_\lambda(t)\rangle = u_\lambda|\phi_\lambda(t+\tau/2)\rangle$ with $u_\lambda \in \{-1,1\}$ and $u_0 \neq u_1$. Using this in Eq. (3) shows that $A^{(0)}_{\lambda\leftarrow\mu} = 0$ for $\lambda \neq \mu$.

[52] J. Gong, L. Morales-Molina, and P. Hänggi, Many-Body Coherent Destruction of Tunneling, Phys. Rev. Lett. **103**, 133002 (2009).

[53] E. S. Mananga and T. Charpentier, Introduction of the Floquet-Magnus expansion in solid-state nuclear magnetic resonance spectroscopy, J. Chem. Phys. **135**, 044109 (2011).

[54] R. Sánchez, G. Platero, and T. Brandes, Resonance fluorescence in driven quantum dots: Electron and photon correlations, Phys. Rev. B **78**, 125308 (2008).

[55] T. Brandes, R. Aguado, and G. Platero, Charge transport through open driven two-level systems with dissipation, Phys. Rev. B **69**, 205326 (2004).

[56] R. Sánchez, G. Platero, and T. Brandes, Resonance Fluorescence in Transport Through Quantum Dots: Noise Properties, Phys. Rev. Lett. **98**, 146805 (2007).

[57] S. Restrepo, J. Cerrillo, V. M. Bastidas, D. G. Angelakis, and T. Brandes, Driven Open Quantum Systems and Floquet Stroboscopic Dynamics, Phys. Rev. Lett. **117**, 250401 (2016).

[58] L. Magazzù, S. Denisov, and P. Hänggi, Asymptotic Floquet states of a periodically driven spin-boson system in the nonperturbative coupling regime, Phys. Rev. E **98**, 022111 (2018).

[59] D. Xu and J. Cao, Non-canonical distribution and non-equilibrium transport beyond weak system-bath coupling regime: A polaron transformation approach, Front. Phys. **11**, 110308 (2016).

[60] C. Duan, Z. Tang, J. Cao, and J. Wu, Zero-temperature localization in a sub-ohmic spin-boson model investigated by an extended hierarchy equation of motion, Phys. Rev. B **95**, 214308 (2017).

[61] C. K. Lee, J. Cao, and J. Gong, Noncanonical statistics of a spin-boson model: Theory and exact Monte Carlo simulations, Phys. Rev. E **86**, 021109 (2012).

[62] G. Engelhardt and J. Cao, Tuning the Aharonov-Bohm effect with dephasing in nonequilibrium transport, Phys. Rev. B **99**, 075436 (2019).